Origin of Near-Infrared Absorption and Large Second Hyperpolarizability in Oxyallyl Diradicaloids: A Three-State Model Approach

K. Yesudas and K. Bhanuprakash*

Inorganic Chemistry Division, Indian Institute of Chemical Technology, Hyderabad-500 007 India

Received: December 23, 2006; In Final Form: January 16, 2007

Bis(benzofuranonyl)methanolate (BM4i4i) dye and croconate dyes (derivatives of oxyallyl molecules) in general are known to have intense transitions in the near-infrared (NIR) region, indicating small transition energies and large transition dipole moments. These molecules have been reported in the literature to have very large resonant third-order nonlinear optical (NLO) susceptibilities and molecular hyperpolarizabilities (γ). In this work we investigate using density functional theory (DFT)/ab initio/symmetry adapted cluster-configuration interaction (SAC-CI) techniques the oxyallyl substructure and attribute the NIR transition and the NLO activity to this substructure, which is common in all these molecules. Using valence bond (VB) theory, an analysis of a three-state model of this substructure is carried out. It is seen that the mixture of an intermediate diradical character and some zwitterionic character in the molecule and a large coupling between these two VB resonance forms is responsible for large γ values. This can be used as a design principle for increasing NLO activity in oxyallyl derivatives.

Introduction

"Functional" dyes are of current research interest as they find applications in optical devices such as optical switches, saturable absorptive mirrors, as materials in electrophotographic reproduction, solar cells, etc.[1−4] They have also been studied extensively for nonlinear optical activity (NLO) for the past two decades and a great deal of attention has been paid to the third-order NLO process, third harmonic generation (THG) because of the potential application in optical limiting, photodynamic therapy, and three-dimensional memories. Recent studies of the organic dyes have concentrated in the absorption range greater than 1000 nm, as these are also useful in telecommunications, medicine, semiconductor lasers, etc.[5−7] As these absorb in the near-infrared region, these dyes are also referred to as NIR dyes.[1] Basically, to absorb in the NIR region, the HOMO−LUMO gap has to be small and this in principle can be obtained through extended π-conjugation or introducing heavy elements in the backbone. But the drawback is that these are labile.[8] Hence, absorption in the NIR region with a smaller chromophore poses a challenge.

A recent study has shown that the BM4i4i dye (Figure 1a) containing an oxyallyl substructure (Figure 1b) absorbs around 1100 nm.[1,2] This absorption is astounding given that the chromophore is small. Langhals analyzed the reason for the large absorption in the red region.[8] It was suggested that the carbenium ion is the acceptor and is based on the Konig and Ismailsky empirical model of D−π−A−π−D (D = donor and A = acceptor)[9−15] absorbance in the longer wavelength region being due to the increased π conjugation. When this acceptor is replaced by squaric acid (Figure 1c), which contains two formal positive charges, the absorption shifts to the red. And on further replacing the squaric acid by the croconic acid (Figure 1d), which is supposed to contain three positive charges, a larger red shift is seen. In addition, BM4i4i's large bathochromic shift has been reasoned to be due to the two carbonyl groups of the lactone rings, which act as "super acceptor groups" to the mesoionic structure and the amino groups (in the figure it is replaced by NH_2) act as the donors. On the basis of this model it was also suggested that the donor groups if replaced by "super donor groups" should result in larger bathochromic effects.[8] Tatsuura et al. suggest that there are two main reasons for this bathochromic shift, one due to the concentration of the π-electrons in the center region of the molecule and the lactone groups acting as the super acceptors and the other due to the twisting of the benzofuranonyl groups.[6] We had shown using the simple orbital interaction picture and high-level calculations like SAC-CI that the red shift occurs not due to the donor acceptor groups but basically due to the smaller interaction in the frontier orbitals.[16]

Interestingly, the third-order NLO susceptibilities determined for the BM4i4i dye are also large and found to be -0.83×10^{-7} esu, an order of magnitude larger than that for polyacetylene.[17] Other very recent NLO experiments by Li et al. suggest that the croconate dyes also have large THG activity, in the resonant conditions, of the same order.[18] The reason for the larger NLO activity was suggested to be due to the good electron acceptance of the croconic acid moiety.[18] Large conjugation, donor acceptor substitutions, and recently suggested diradical character are normally the major reasons for large NLO activity.[19−21] In the latter type, which is of interest here, it has been postulated that the electrons, which are not having a large bonding character are sensitive to the applied field and this leads to large fluctuations of electrons or large polarization.[20] With this model, many molecules like imidazole, triazole rings, and polycyclic aromatic hydrocarbons involving phenalenyl radical molecules have been predicted to have large γ values.[21]

To understand the actual origin of the large γ value and NIR absorption in the BM4i4i dye and suggest a general design principle for the oxyallyl based systems are the main aims of this work. We have divided the paper as follows. In the first section we discuss the singlet and triplet geometries of the simple oxyallyl substructures, including the relative energy differences of the singlet and triplet. In the next section we show how the absorption can be enhanced by geometry perturbation. Next we discuss the SAC/SAC-CI and three-state model of the γ values, followed by γ values evaluation of the BM4i4i dye

* Corresponding author. E-mail: bhanu2505@yahoo.co.in.

10.1021/jp068900a CCC: $37.00
Published on Web 02/21/2007

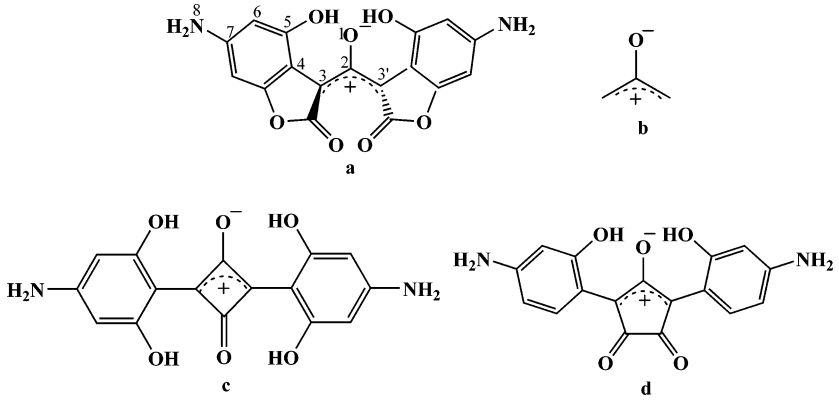

Figure 1. Structures of (a) bis(benzofuranonyl)methanolate (BM4i4i), (b) oxyallyl, (c) squaraine, and (d) croconate dyes.

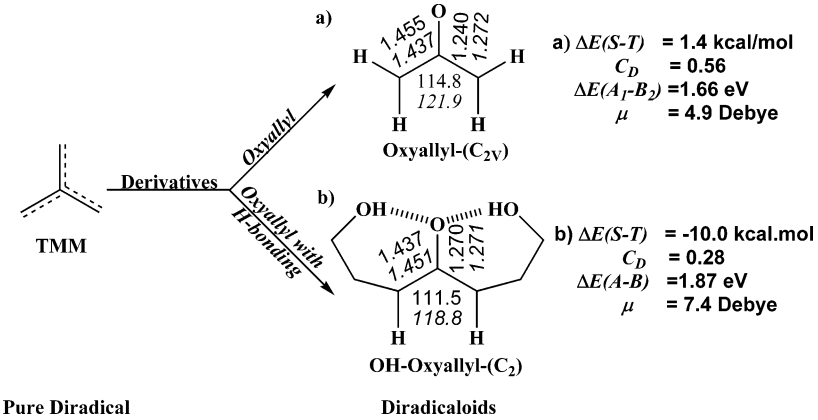

Figure 2. Schematic diagram of perturbation of TMM to its derivatives by substitution of a heteroatom and important properties for the singlet and triplet states. The important geometric parameters and dipole (μ), diradical character (C_D) and transition energies $\Delta E(A_1-B_2$ and $A-B)$ are obtained from B3LYP/6-31G(d), UHF/6-31+G(d,p), and SAC/SAC-CI/6-31G(d,p) respectively. The geometric parameters for the triplet state are given in italics.

by SOS and FF methods. We derive, using the VB three-state model of the oxyallyl substructure, the energy and transition dipole and show the actual origin of the small absorption energies.

Computational Methods

All calculations have been carried out using the G03W software.[22] The DFT B3LYP methods are used for optimization of all the molecules studied here. We have carried out the optimizations in the broken spin symmetry wave function (unrestricted) (Guess=Mix option) and restricted wave function. For the optimizations, we use 6-31G(d,p) basis with polarization, and for properties, in some cases we have also added diffuse functions, i.e., 6-31+G(d,p) and 6-31++G(d,p). The detailed geometrical parameters and vibrational frequencies are given in the Supporting Information. The geometries obtained using these two methods have then been subjected to the SAC/SAC-CI[23] calculations using G03W. For the ground state SAC is carried out and it is nonvariational, whereas for the excited state SAC-CI is carried out using the variational methods.[23] The full active space is chosen for all the molecules except for BM4i4i dye; here an active space with the window option in which some core and some virtual MOs are not used and have at least 160 orbitals for the excitations are chosen. To the ground state all the single excitation operators in this are included without selection. For the doubles-excitation operators an energy threshold value of 5.0×10^{-6} hartree is used to select the configurations based on a perturbation method.

SAC-CI is also restricted to singles and doubles linked operators, but the higher order ones are treated through unlinked operators. For each molecule four lowest excited states are calculated. The double excitation operators selection of the configurations is again based on a perturbation approach. Here the interaction with the reference states is carried out and any configuration that has an interaction energy greater than a threshold value of 5.0×10^{-7} hartree is selected. Raising the threshold to 1.0×10^{-5} hartree for the SAC and 1.0×10^{-6} hartree for the SAC-CI brings about a change in the absorption energy of a maximum of 0.1 eV; hence the convergence is nearly achieved.

Results and Discussions

(a) Oxyallyl and OH-Oxyallyl Substructures. *Energy and Geometry.* Simple oxyallyl is a derivative of the trimethylmethane (TMM) (Figure 2), which is known to be a pure diradical.[24] Thus a diradicaloid character can be expected in the oxyallyl molecule. In fact, the ground state of the unsubstituted oxyallyl is a triplet.[25,26] To obtain the lowest singlet state geometry and energy, a multideterminant wave function has to be used.[25,26] Recently, Hess et al. obtained the singlet state of this molecule using the unrestricted DFT methods by mixing up the spin orbitals to obtain the broken spin-symmetry wave function in the single determinant theory.[26] They showed that the energy and geometry obtained by this method is equal to the multideterminant approach. Such a calculation carried out at the unrestricted-B3LYP/6-31G(d) level yields a value of 1.4 kcal/mol for the singlet−triplet gap, with the singlet being higher in energy. The S^2 value is around 0.836. As we are also interested in properties like dipole moment, we repeat the calculations of oxyallyl at the same level here. The details are shown in Figure 2.

H-bonded oxyallyl (OH-oxyallyl) is a common substructure in the oxyallyl based dyes including the BM4i4i dye. Hence

we carry out the studies on this substructure here. This is also carried out with the intention of comparing properties with the unsubstituted oxyallyl substructure. We create a H-bond in the simple oxyallyl substructure by taking up a moiety with CH_2-CH_2-OH substitution, as shown in Figure 2b. We obtain the geometry and energy of this H-bonded oxyallyl (which should also have an intermediate diradical character) using the broken spin symmetry unrestricted DFT (B3LYP/6-31G(d)) methods in the single determinant theory for both the singlet and triplet. The geometry obtained differs from the oxyallyl molecule. Here the C−O bond is lengthened considerably to 1.27 Å from 1.24 Å in the oxyallyl and the $C_3-C_2-C_{3'}$ bond angle is at 114.8° compared to 111.5° in the oxyallyl molecule. The C−C bond length changes by 0.02 Å. The S^2 value is 0.428. The major difference in this case is that the singlet state is lower in energy than the triplet state and the ΔE(S−T) gap reveals that the triplet state is unstable by around 10 kcal/mol. As for the properties, there is a larger dipole moment of 7.4 D compared to 4.9 D for the oxyallyl molecule. The restricted DFT methods applied to this molecule do not predict a minimum for this molecule also, and we obtain an imaginary (negative) frequency. The energy obtained in this method is also slightly higher by 1.6 kcal/mol.

Diradical Character. As the diradical nature is quite large, it would be of interest to estimate this character for comparison. Several methods have been suggested for estimating the diradical character.[27−30] Wirz had suggested that a molecule can be said to be a diradical if the splitting between the singlet (S_0) and triplet (T_1) is around 2−24 kcal/mol.[27a] From this method one can see that the oxyallyl and OH-oxyallyl due to their small singlet−triplet splittings can be considered as diradicaloids. On the other hand the percent diradical character can also be estimated by using the method suggested by Nakano et. al.[28] Here it is related to the HOMO$-i$ and LUMO$+i$ and is defined as the weight of doubly excited configuration in the MC-SCF theory and is formally expressed in the spin-projected UHF-(PUHF) theory as[29,30]

$$C_D = \left(1 - \frac{2S_i}{1 + S_i^2}\right) \times 100 \qquad (1)$$

where S_i is the orbital overlap (χ_{HOMO-i} and η_{HOMO-i}) between the corresponding pairs

$$\chi_{HOMO-i} = \cos(\omega)\phi_{HOMO-i} + \sin(\omega)\phi_{LUMO+i}$$

and

$$\eta_{HOMO-i} = \cos(\omega)\phi_{HOMO-i} - \sin(\omega)\phi_{LUMO+i}$$

Here ω and ϕ represent the UHF natural orbital (UNO) and orbital mixing parameter, respectively. The orbital overlap can be replaced by the occupation numbers (n_j) of UNOs, which are obtained from the density matrix. This has been shown to be suitable.[27b] Therefore S_i can be expressed as

$$S_i = \frac{n_{HOMO-i} - n_{LUMO+i}}{2}$$

It has been found in earlier studies that diradical character estimated by the unrestricted DFT methods is underestimated whereas the ab initio UHF methods give reasonable diradical character.[31] Of the DFT methods for estimation of intermediate diradical character the UBHandHLYP method seems reasonable[21] because it contains 50% HF, i.e.,[22]

$$\text{UBHandHLYP} = 0.5E_X^{HF} + 0.5E_X^{LSDA} + 0.5\Delta E_X^{Becke88} + E_C^{LYP}$$

Hence in this work we estimate the diradical character by the UHF and UBHandHLYP methods only. The diradical character calculated using this formula shows that the oxyallyl molecule in its minimized singlet state has a large diradical character of 0.56 whereas the OH-oxyallyl shows an intermediate diradical character of 0.28.

Variation of the Diradical Character. Large diradical character leads to large γ values;[20,21] hence our interest is to see the variation of the diradical character and its effect on properties. This is achieved by geometry perturbation. The rationale behind this is that the oxyallyl substructure in many classes of dyes has a different $C_3-C_2-C_{3'}$ bond angle.[16] Examining the MOs of the lowest singlet state of the two molecules, one sees that the HOMO and the LUMO in Figure 3 are of a and b character. The LUMO is a pure NBO. Decreasing the HOMO−LUMO gap would increase the involvement of this orbital in the wave function and lead to larger diradicaloid character.[32−34] This could be achieved by increasing the angle $C_3-C_2-C_{3'}$ of the substructure, which would simply decrease the interaction between the two dominant atomic orbitals.[16b] We carry out single point calculations at the unrestricted B3LYP/6-31+G-(d,p) level for each angle and estimate the diradical character by the methods outlined above. The variation of the bond angle and the estimated diradical character by the two methods (UHF and UBHandHLYP) is shown graphically in Figure 4a for both the moieties. Clearly the diradical character increases with widening of the angle in both molecules. In the OH-oxyallyl case the diradical character increases only up to 0.35 from 0.2 (angle variation is 100−125°), but in the case of oxyallyl it increases from 0.25 to 0.7 (angle variation is again 100−125°). As mentioned above, the UBHandHLYP method shows a smaller diradical character but the trends remain same.

We now study the effect of the lengthening of the C−O bond on the diradical character. For this we elongate the C−O bond of the oxyallyl molecule from 1.20 to 1.44 Å at 0.1 Å intervals and calculate the diradical character of the molecule using eq 1. We see a small decrease in the diradical character of the molecule with elongation of the C−O bond. This is shown in Figure 4b.

Transition Energy. To understand the effect of the diradical character on the transition energies of both oxyallyl and OH-oxyallyl substructure, we carry out SAC-CI calculations at each single point, with increasing diradical character (widening of $C_3-C_2-C_{3'}$ angle). The lowest singlet state is a $^1A_1$ state in oxyallyl and ^1A in OH-oxyallyl in which the HOMO is doubly occupied whereas the first excited state ($^1B_1$) involves the a−b transition into the LUMO. The final state (A_1) is again a doubly occupied $^1A_1$ state. The SAC-CI details are given in Table 1. The lowest state is calculated at the nonnvariational SAC level.[23] The calculation has been carried out with the no window option (full active space) and with the selection of the lowest four states in each symmetry. The coefficients of the dominant configurations are given in Table 2. As we are carrying out the SAC-CI calculations, some smaller configurations of the same symmetry mix up in the CI. Due to this in the OH-oxyallyl case we find that the doubly excited state need not be the 2A state. In most of the cases in the OH-oxyallyl it is the fourth one. In the table the oscillator strengths of the transition from the SAC ground state $^1A_1(^1A)$ to the first excited state $^1B_2(^1B)$ state is shown. Recalculated oscillator strengths from the $^1B_2(^1B)$ state to the target excited $^1A_1(^1A)$ states are shown in the same table. It is clearly seen that only the transition to the doubly excited configuration *A* state has a large oscillator strength.

The energy of transition calculated from the lowest singlet state ($^1A_1$) to ($^1B_2$) in the C_{2v} symmetry at the SAC-CI level for the minima of the oxyallyl molecule is 1.66 eV. ΔE(transition) between ^1A and ^1B of the minimized OH-oxyallyl molecule is around 1.87 eV quite close to the oxyallyl molecule's value. As the diradical character increases, the lowest energy of transition also red shifts, which is shown for both the molecules in Figure 5. For the oxyallyl molecule the red shift takes place much slower and reaches 1 eV at the diradical character of 0.7. In the case of the OH-oxyallyl molecule the value reaches 1 eV at 0.35. The geometry in both these cases are nearly the same (angle). The oscillator strength for both the molecules decreases with an increase in diradical character, as seen in Figure 5. An important difference here is that the OH-oxyallyl molecule has a larger oscillator strength in general. Due to this we expect that the OH-oxyallyl substructure based molecule without the H-bond would lead to larger γ values. As we move on to the γ calculations, our discussions pertain only to the OH-oxyallyl systems and not the simple oxyallyl moiety whose ground state is actually a triplet.

(b) Second Hyperpolarizability. *General Theoretical Background.* When a molecule is exposed to a medium with an optical electric field, it becomes polarized. At the microscopic level, the response can be expressed as a function of dipole and energy as

$$\mu_i(F) = \mu_i(0) + \alpha_{ij}F_j + \frac{1}{2}\beta_{ijk}F_jF_k + \frac{1}{6}\gamma_{ijkl}F_jF_kF_l + \ldots \quad (2)$$

$$E(F) = E(0) - \mu_iF_i - \frac{1}{2}\alpha_{ij}F_iF_j - \frac{1}{6}\beta_{ijk}F_iF_jF_k - \frac{1}{24}\gamma_{ijkl}F_iF_jF_kF_l + \ldots \quad (3)$$

where $\mu_i(0)$, is its permanent dipole, $E(0)$ is the energy of the molecule in the absence of electric field, α_{ij} is the dipole polarizability, and β_{ijk} and γ_{ijkl} are first and second hyperpolarizability tensors, respectively, obtained as first-, second-, and third-order derivatives of dipole moment μ_i with respect to the applied field F; i.e., the nth order polarizability can be expressed as the nth-order derivative of dipole moment or the $(n+1)$th derivative of the total energy because the dipole moment is the negative first-order derivative of molecular total energy.

$$\alpha_{ij} = \left(\frac{\partial\mu_i}{\partial F_j}\right)_{F=0}$$

$$\beta_{ijk} = \left(\frac{\partial^2\mu_i}{\partial F_j\partial F_k}\right)_{F=0}$$

$$\gamma_{ijkl} = \left(\frac{\partial^3\mu_i}{\partial F_j\partial F_k\partial F_l}\right)_{F=0}$$

Basically, there are two commonly used techniques to calculate the polarizabilities. The first one is the sum-over-states (SOS) method and the other is finite-field (FF) method.

SOS Method. In this section we briefly describe the structure−property co-relation based on the perturbative treatment. The perturbational equation for γ can be written as[19,35]

$$\gamma_{iiii} = 24\sum_{n\neq g}\left[\frac{(\mu^i_{ng}\Delta\mu^i_{ng})^2}{(E_{ng})^3} - \frac{(\mu^i_{ng})^4}{(E_{ng})^3} + \sum_{m\neq n,g}\frac{(\mu^i_{ng})(\mu^i_{nm})^2}{(E_{ng})^2E_{mg}}\right]$$

$$\gamma_{iijj} = 4\sum_{n\neq g}\left[\frac{4\mu^i_{ng}\mu^j_{ng}\Delta\mu^i_{ng}\Delta\mu^j_{ng} + (\mu^i_{ng}\Delta\mu^j_{ng})^2 + (\mu^j_{ng}\Delta\mu^i_{ng})^2}{(E_{ng})^3} - \frac{6(\mu^i_{ng}\mu^j_{ng})^2}{(E_{ng})^3} + \sum_{m\neq n,g}\frac{4\mu^i_{ng}\mu^i_{mn}\mu^j_{ng}\mu^j_{mn} + (\mu^i_{ng}\mu^j_{mn})^2 + (\mu^j_{ng}\mu^i_{mn})^2}{(E_{ng})^2E_{mg}}\right] \quad (4)$$

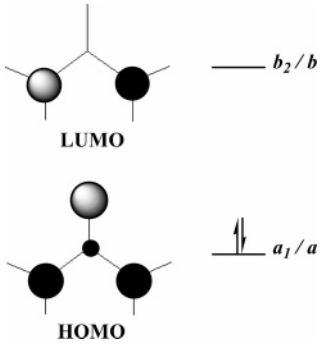

Figure 3. Frontier one electron molecular orbitals of oxyallyl/OH-oxyallyl substructure.

where $i = x, y, z$. Here the parameters μ_{ng} and μ_{nm} correspond to the transition moments between the ground and the nth excited state, and nth excited to mth excited states. $\Delta\mu_{ng}$ is the difference in dipole moments between the ground and the nth excited states. Similarly, E_{ng} and E_{mg} correspond to the energy of transition between the ground and the n/mth-excited state.

In the three-state model approximation (ground (A), excited state (B), and the final state (A))[35] and using the symmetry arguments (e.g., $\Delta\mu^y_{ng}$ is zero and transition dipole moments in Z being zero and in X being very small), we obtain only the following longitudinal major component for our case here,

$$\gamma_{yyyy} = 24\sum_{n\neq g}\left[-\frac{(\mu^y_{^1B_2,^1A_1})^4}{(E_{^1B_2,^1A_1})^3} + \sum_{m\neq n,g}\frac{(\mu^y_{^1B_2,^1A_1})(\mu^y_{^2A_1,^1B_2})^2}{(E_{^1B_2,^1A_1})^2E_{^2A_1,^1B_2}}\right] \quad (5)$$

or in other words $\gamma^T = \gamma^2 + \gamma^3$ where the first term in eq 5 is γ^2 and the positive term is γ^3. In the above expression if the first term dominates, then a negative value is obtained and if second term dominates, a positive value is obtained. From the equation it is also clear that when the transition dipole moment is large and the transition energy is small the γ^2 value increases.

SOS three-state method has been used earlier by other workers to understand the actual transitions responsible for the origin of γ in the molecule[20,35a] We use this SOS three-state model here for understanding the second-order hyperpolarizability of the OH-oxyallyl system. We determine the transition energy of the ground state to the first excited state and excited state to the final state using the SAC-CI methods. The transition dipole moment is also determined by the same methods. We evaluate the γ for each point with changing the angle. Clearly with increasing the angle/diradical character there is an increase in the γ value, which is shown in Figure 6. The γ value is also very large indicating that even this small moiety without any substitution can show a very high value of 2.6×10^5 au when the diradical character is 0.38. The detailed results are shown in Table 3. The γ^T values and γ^2 values behave similarly in Figure 6 and are nearly equal, indicating the dominance of γ^2 term in the total γ.

(c) Hyperpolarizability of BM4i4i Dye. *Geometry and Energy.* We now extended the studies to the singlet state of the BM4i4i dye. The BM4i4i dye is optimized in the restricted and

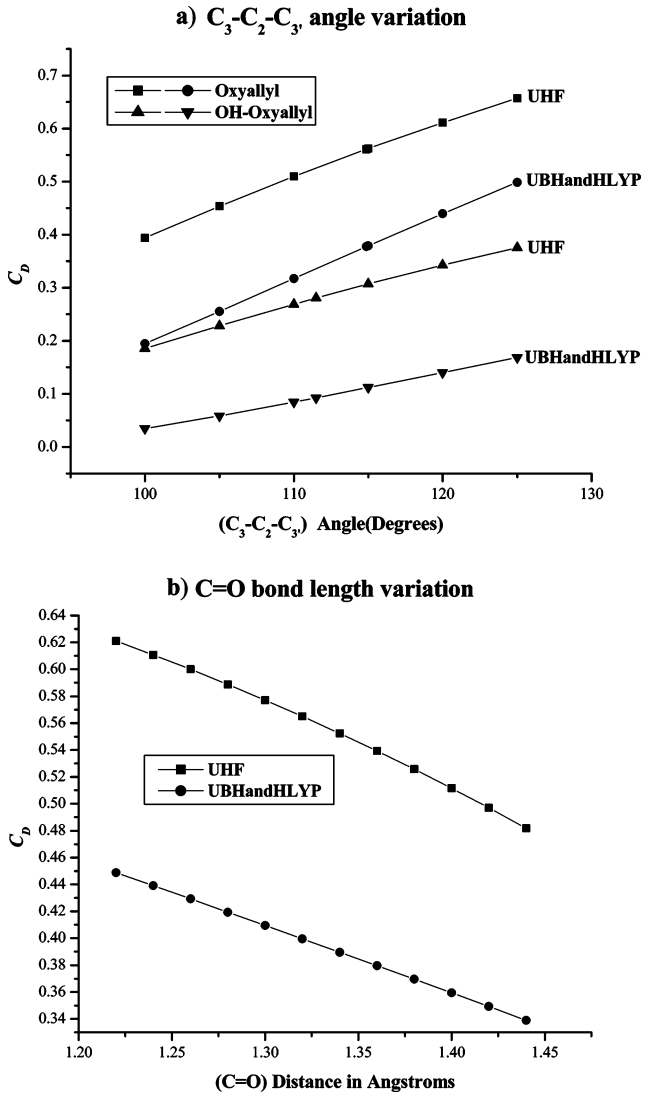

Figure 4. Diradical character (C_D) variation due to geometry perturbation of the singlet oxyallyl/OH-oxyallyl calculated at the UHF and UBHandHLYP/6-31+G(d,p) levels.

the spin unrestricted methods. We use the DFT-B3LYP/6-31G-(d,p) and unrestricted B3LYP/6-31G(d,p) methods. The energies and geometries are shown in Table 4. We notice that with the restricted method we obtain a stable minima with positive (real) frequencies unlike the oxyallyl or OH-oxyallyl case. The energy difference between the B3LYP and unrestricted B3LYP is also very small and is only 0.5 kcal/mol. There is only a very slight variation of the geometry obtained in the two methods (Table 4). But on the other hand the unrestricted method shows a S^2 value of 0.4, compared to the restricted methods S^2 value of 0.

SOS Method. We now calculate the γ value using the SOS three-state model. The SAC-CI calculations have been carried out at the restricted methods optimized geometry using the 6-31G(d,p) basis set. The generated configuration is 6054061 and selected is 28752 for the 1^1A state and for the 3^1A the generated/selected is 6056520/105418. In the case of the singly excited state 1B the generated/selected is 6054060/101820. The energy of transition from the ground state to the first excited state is 1.04 eV and the transition dipole moment is 12.6 D. The excitation from the singly excited state to the doubly excited state is 1.89 eV and transition dipole moment is 5.5 D. Using these values in eq 5, we obtain $\gamma^2 = -4.2 \times 10^7$ au, $\gamma^3 = 2.8 \times 10^6$ au and the total γ is -3.9×10^7 au. This indicates that γ is fairly high.

Finite Field (FF) Method. The FF method is based on numerical differentiation and field dependent. Hence the Hamiltonian in FF contains an extra term, i.e., the interaction between external static field and the molecular system.[19]

$$\hat{H}(F) = \hat{H}_0 - \sum Fr$$

The molecules lie in *YZ* plane and stretch toward the *Y* axis, so that γ_{yyyy}, in most cases dominate the isotropic average γ defined as[19]

$$\langle\gamma\rangle = \frac{1}{5}(\gamma_{xxxx} + \gamma_{yyyy} + \gamma_{zzzz} + 2\gamma_{xxyy} + 2\gamma_{xxzz} + 2\gamma_{yyzz})$$

and hence we only concentrate on the longitudinal hyperpolarizability (γ_{yyyy}).

The static dipole hyperpolarizabilities of these molecules are evaluated using numerical finite-field methods. The detailed individual hyperpolarizabilities γ_{iiii} of the dipole moments and the static dipole hyperpolarizability components in terms of the finite field energies are[35a]

$$\gamma_{iiii} = \{-56E(0) + 39[E(F_i) + E(-F_i)] - 12[E(2F_i) + E(-2F_i)] + [E(3F_i) + E(-3F_i)]\}/6F_i^4 \quad (6)$$

where the $E(Fi)$ represent energies in presence of the perturbing fields, F, directing along the i axis that correspond to the y Cartesian coordinates. We have used a four-point procedure for evaluating γ_{yyyy} at the field strength values of 0.0, 0.005, 0.010, and 0.015 au, for the smaller basis sets. Comparison of γ values obtained by the three-point formula[35b] and four-point formula for the smaller basis sets shows that they are almost same (shown in Supporting Information). Keeping in view the saving of computer time, we used the three-point formula for larger basis sets.

We use the geometry obtained using the restricted methods to avoid the problem with spin contamination and carry out the

TABLE 1: Dimensions of the Linked Operator and Configurations in the SAC/SAC-CI Calculations for Minimized Oxyallyl and OH-Oxyallyl

	SAC				SAC-CI			
molecule	state[a]	before[b]	after[c]	no. of configurations[d]	state[a]	before[b]	after[c]	no. of configurations[d]
oxyallyl	A1	69741	15018	14	A1	69741	21720	19
					A2	58784	21377	
					B1	58976	19348	
					B2	69184	19474	16
OH-oxyallyl	A	6152883	46151	5	A	6152883	116248	18
					B	6150396	99624	13

[a] Number of solutions for SAC is 1; for SAC-CI it is 4. [b] Number of linked operators before selection. [c] Number of linked operators after selection. [d] Number of configurations that have a CI coefficient larger than 0.03.

TABLE 2: Mixing Coefficients for the Ground, Excited, and Final States (A_1/A, B_2/B, and A_1/A) Obtained from SAC/SAC-CI at the 6-31G(d,p) Basis for Oxyallyl and OH-Oxyallyl

(a) Oxyallyl

angle (deg)	state	main configurations ($\|c\| \geq$ **0.15**	ΔE (eV)	f
100	$1B_2$	$0.85(15B_1-16A_2) + 0.38(13B_1-16A_2) - 0.33(15B_1-18B_1;15B_1-16A_2)$	2.29	0.072
	$1A_1$	$0.50(15B_1-18B_1) + 0.36(13B_1-18B_1) + 0.28(14B_2-20B_2) + 0.15(14B_2-21B_2) +$ **$0.57(15B_1-16A_2;15B_1-16A_2)$** $- 0.40(15B_1-16A_2;13B_1-16A_2)$	7.42	0.484
105	$1B_2$	$0.85(15B_1-16A_2) + 0.39(13B_1-16A_2) - 0.33(15B_1-18B_1;15B_1-16A_2)$	2.09	0.069
	$1A_1$	$-0.56(15B_1-18B_1)-0.36(13B_1-18B_1) - 0.28(14B_2-20B_2) - 0.15(14B_2-21B_2) -$ **$0.55(15B_1-16A_2;15B_1-16A_2)$** $+ 0.38(15B_1-16A_2;13B_1-16A_2)$	7.48	0.517
110	$1B_2$	$0.85(15B_1-16A_2) + 0.39(13B_1-16A_2) - 0.33(15B_1-18B_1;15B_1-16A_2)$	1.85	0.063
	$1A_1$	$0.56(15B_1-18B_1) + 0.34(13B_1-18B_1) + 0.30(14B_2-20B_2) + 0.15(14B_2-21B_2) +$ **$0.53(15B_1-16A_2;15B_1-16A_2)$** $- 0.36(15B_1-16A_2;13B_1-16A_2)$	7.53	0.530
114.88	$1B_2$	$0.85(15B_1-16A_2) + 0.40(13B_1-16A_2) - 0.34(15B_1-18B_1;15B_1-16A_2)$	1.66	0.058
	$1A_1$	$0.57(15B_1-18B_1) + 0.34(13B_1-18B_1) + 0.32(14B_2-20B_2) +$ **$0.51(15B_1-16A_2;15B_1-16A_2)$** $- 0.35(15B_1-16A_2;13B_1-16A_2)$	7.59	0.559
115	$1B_2$	$-0.85(15B_1-16A_2) - 0.40(13B_1-16A_2) + 0.34(15B_1-18B_1;15B_1-16A_2)$	1.65	0.058
	$1A_1$	$0.57(15B_1-18B_1) + 0.34(13B_1-18B_1) + 0.32(14B_2-20B_2) +$ **$0.51(15B_1-16A_2;15B_1-16A_2)$** $- 0.35(15B_1-16A_2;13B_1-16A_2)$	7.60	0.560
120	$1B_2$	$0.85(15B_1-16A_2) + 0.40(13B_1-16A_2) - 0.34(15B_1-18B_1;15B_1-16A_2)$	1.45	0.053
	$1A_1$	$0.59(15B_1-18B_1) + 0.34(13B_1-18B_1) + 0.33(14B_2-20B_2) +$ **$0.50(15B_1-16A_2;15B_1-16A_2)$** $- 0.34(15B_1-16A_2;13B_1-16A_2)$	7.66	0.588
125	$1B_2$	$-0.85(15B_1-16A_2) - 0.40(13B_1-16A_2) + 0.34(15B_1-18B_1;15B_1-16A_2)$	1.28	0.048
	$1A_1$	$0.60(15B_1-18B_1) + 0.34(14B_2-20B_2) + 0.33(13B_1-18B_1) +$ **$0.49(15B_1-16A_2;15B_1-16A_2)$** $- 0.32(15B_1-16A_2;13B_1-16A_2)$	7.69	0.609

(b) OH-Oxyallyl

angle (deg)	state	main configurations ($\|c\| \geq$ **0.15**	ΔE[a] (eV)	f[b]
100	1B	$0.90(39B-40A) + 0.22(33B-40A) + 0.24(39B-42B;39B-40A)$	2.46	0.166
	1A	$-0.94(37A-40A)$	1.45	0.001
	2A	$0.94(34B-40A)$	3.43	0.014
	3A	$0.76(38B-42B) + 0.38(38B-43B) - 0.28(36B-42B) + 0.16(38B-47B) + 0.29(39B-40A;38B-40A)$	4.12	0.000
	4A	$0.60(39B-42B) + 0.34(30B-40A) + 0.29(39B-43B) +$ **$0.30(39B-40A;39B-40A)$**	4.95	0.114
105	1B	$0.90(39B-40A) + 0.23(33B-40A) + 0.22(39B-42B;39B-40A) + 0.15(39B-43B;39B-40A)$	2.20	0.150
	1A	$0.94(37A-40A)$	1.49	0.001
	2A	$0.94(34B-40A)$	3.55	0.016
	3A	$0.72(38B-42B) + 0.42(38B-43B) - 0.26(36B-42B) + 0.18(38B-47B) - 0.16(36B-43B) + 0.33(39B-40A;38B-40A)$	4.49	0.000
	4A	$0.53(39B-42B) + 0.33(30B-40A) + 0.29(39B-43B) + 0.21(31A-40A) +$ **$0.32(39B-40A;39B-40A)$**	5.05	0.161
110	1B	$0.89(39B-40A) + 0.23(33B-40A) - 0.22(39B-42B;39B-40A) - 0.16(39B-43B;39B-40A)$	1.94	0.134
	1A	$-0.94(37A-40A)$	1.57	0.000
	2A	$0.79(29A-40A) + 0.37(31B-40A) - 0.29(30A-40A)$	3.92	0.003
	3A	$-0.93(35A-40A)$	3.52	0.014
	4A	$-0.43(39B-42B) + 0.42(30B-40A) + 0.33(31A-40A) - 0.26(39B-43B) +$ **$0.29(39B-40A;39B-40A)$**	5.24	0.198
111.5	1B	$-0.89(39B-40A) - 0.23(33B-40A) + 0.21(39B-42B;39B-40A) + 0.16(39B-43B;39B-40A)$	1.87	0.129
	1A	$-0.94(37A-40A)$	1.57	0.000
	2A	$-0.81(30A-40A) - 0.40(31B-40A) - 0.19(29A-40A)$	3.91	0.002
	3A	$0.92(35A-40A)$	3.50	0.014
	4A	$0.41(31B-40A) - 0.39(39B-42B) - 0.32(30B-40A) + 0.30(29A-40A) - 0.24(39B-43B) +$ **$0.28(39B-40A;39B-40A)$**	5.20	0.194
115	1B	$0.89(39B-40A) + 0.23(33B-40A) - 0.21(39B-42B;39B-40A)$	1.72	0.119
	1A	$-0.94(37A-40A)$	1.60	0.000
	2A	$-0.75(30A-40A) - 0.50(31B-40A) + 0.23(35A-40A)$	3.84	0.003
	3A	$0.90(35A-40A) + 0.20(30A-40A)$	3.44	0.013
	4A	$0.58(31A-40A) - 0.42(30B-40A) - 0.28(39B-42B) + 0.25(24A-40A) - 0.17(39B-43B) +$ **$0.21(39B-40A;39B-40A)$** $- 0.17(39B-40A;32B-40A)$	5.33	0.125
120	1B	$-0.89(39B-40A) - 0.24(33B-40A) + 0.21(39B-42B,39B-40A) + 0.15(39B-43B,39B-40A)$	1.50	0.104
	1A	$0.94(37A-40A)$	1.64	0.000
	2A	$0.66(31B-40A) + 0.57(30A-40A) - 0.31(35A-40A)$	3.85	0.005
	3A	$0.88(35A-40A) + 0.23(31B-40A) + 0.22(30A-40A)$	3.38	0.012
	4A	$-0.59(30B-40A) + 0.48(31A-40A) + 0.25(24A-40A) - 0.22(39B-42B) + 0.19(39B-40A,39B-40A) -$ **$0.17(39B-40A,32B-40A)$**	5.42	0.120
125	1B	$0.89(39B-40A) + 0.23(33B-40A) + 0.21(39B-42B;39B-40A)$	1.31	0.091
	1A	$0.94(37A-40A)$	1.68	0.000
	2A	$0.75(32A-40A) - 0.39(35A-40A) + 0.37(30A-40A)$	3.82	0.006
	3A	$0.85(35A-40A) + 0.34(32A-40A) + 0.21(30A-40A)$	3.30	0.010
	4A	$0.71(30B-40A) - 0.35(32B-40A) - 0.26(24A-40A) - 0.19(39B-42B) -$ **$0.17(39B-40A;39B-40A)$** $+ 0.16(39B-40A;31A-40A)$	5.57	0.098

[a] ΔE is with respect to the ground state. [b] Oscillator strengths (ground state A−B) and (excited state B−A).

finite field studies (restricted FF). The γ values obtained using various methods are shown in Table 5. We see the γ value is very large and has a good agreement with values obtained by three-state SOS methods. We obtain γ^T of -3.9×10^7 au in the SOS method, but in the FF method it is -0.35×10^7 au. In the RHF methods the values are around 10 times larger. The values are in good agreement with those obtained by different basis sets and methodologies.

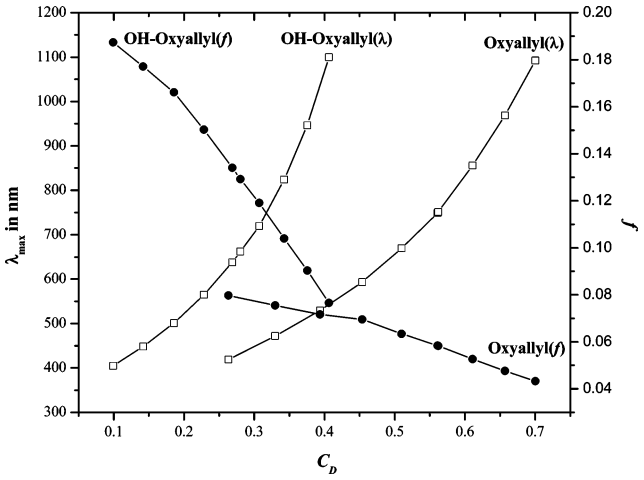

Figure 5. Variation of λ_{max} (nm) and oscillator strengths (f) with diradical character (C_D) Calculated by SAC/SAC-CI at the 6-31G(d,p) basis.

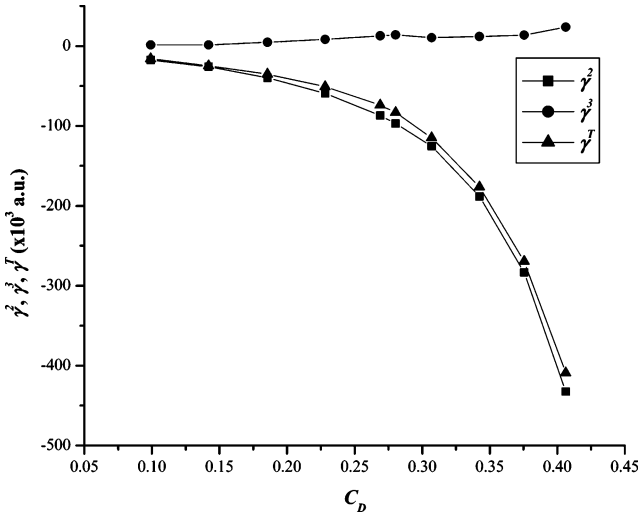

Figure 6. Variation of the longitudinal component of $\gamma(\gamma^2, \gamma^3, \gamma^T$ au) with diradical character (C_D) for singlet OH-oxyallyl calculated by SAC/SAC-CI at the 6-31G(d,p) Basis.

TABLE 3: Diradical Character (C_D), γ_{yyyy} (γ^2, γ^3, γ^T),[a] Excitation Energies (ΔE_{ge} and ΔE_{gf}, in eV), and Transition Moments (μ_{ge} and μ_{ef}, in Debye) for Different Bond Angles (deg) of Singlet OH-Oxyallyl Calculated by SAC/SAC-CI at 6-31G(d,p) Basis

angle	C_D	ΔE_{ge}	ΔE_{gf}	μ_{ge}[b]	μ_{ef}[b]	γ^2	γ^3	γ^T
100	0.1856	2.48	7.43	4.206	2.461	−39835	4544	−35291
105	0.2283	2.20	7.25	4.248	2.895	−59336	8351	−50985
110	0.2689	1.94	7.18	4.262	3.159	−86789	12902	−73887
111.5	0.2804	1.87	7.07	4.264	3.140	−97139	13957	−83181
115	0.3070	1.72	7.05	4.269	2.483	−125324	10363	−114961
120	0.3425	1.50	6.92	4.269	2.311	−188427	12003	−176424
125	0.3755	1.31	6.88	4.262	2.152	−283295	13750	−269545

[a] The γ values are given in a.u. (1 au = 5.0367×10^{-40} esu). [b] Only y component is nonzero due to symmetry.

(d) Valence Bond−Three-State Model. *Diradical Character.* To understand the behavior in these systems, we make use of the valence bond theory. The OH-oxyallyl molecules can be modeled by assuming the resonance between two zwitterionic forms and a diradical form (Figure 7) (a three-state model). For comparison the resonance structures of the oxyallyl are also given. An important difference we notice is that the OH-oxyallyl can still have a zwitterionic character even in the dominant diradical form. The two zwitterionic forms are degenerate, as shown in the same figure. The corresponding wave functions are Φ_{Z1}, Φ_{Z2} and Φ_D. The coupling between the zwitterionic states is given as T and the coupling between the diradical form and any zwitterionic form is t. The Hamiltonian can be written in this basis as[36−42]

TABLE 4: Optimized Important Geometrical Parameters (Å and deg) for BM4i4i-Dye Calculated at DFT/6-31G(d,p)

geometry parameters	methodologies	
	B3LYP[a]	UB3LYP[a,b]
O_1-C_2	1.305	1.296
C_2-C_3	1.424	1.431
C_3-C_4	1.407	1.408
C_4-C_5	1.436	1.435
C_5-C_6	1.395	1.393
C_6-C_7	1.409	1.409
C_7-N_8	1.363	1.364
O_1-H (H-bond)	1.542	1.572
$O_1-C_2-C_3$	119.3	119.3
$C_2-C_3-C_4$	127.7	127.7
$C_3-C_2-C_{3'}$	121.3	121.5

[a] The energies obtained are −1289.936979/−1289.937848 au at B3LYP/UB3LYP and the relative energy difference ($E_{UB3LYP} - E_{B3LYP}$) is 0.5 kcal/mol. [b] $S^2 = 0.4153$ at UB3LYP.

TABLE 5: Molecular Longitudinal Second Hyperpolarizabilities (γ_{yyyy})[a] of Pure Singlet State Molecules Calculated by the Finite Field Method at the B3LYP/6-31G(d,p) Optimized Geometries

method	basis set			
	6-31+G(d,p)	6-31++G(d,p)[b]	cc-pVDZ	cc-pVTZ[b]
		BM4i4i		
RHF	−16423413	−10428480	−14960213	−10677440
RB3LYP	−1606720	−1576640	−1379307	−1525760
RB3PW91	−1593120	−1570240	−1392747	−1537600
RBHandH	−3527467	−3267200	−3009867	−3179840
RBHandHLYP	−3507413	−3247360	−3014987	−3179840

[a] The γ values are given in au (1 au = 5.0367×10^{-40} esu). [b] Obtained using three-point formula for γ[35b].

$$\begin{bmatrix} E_D & -t & -t \\ -t & E_Z & -T \\ -t & -T & E_Z \end{bmatrix}$$

Here E_D denotes the electronic energy of the diradical state and E_Z for the two degenerate zwitterionic states. Diagonalizing this matrix, the eigenvalues and eigen vectors are obtained as[36]

$$E_g = \frac{1}{2}[E_D + E_Z - T] - \frac{1}{2}[(\Delta E_{ZD} - T)^2 + 8t^2]^{1/2}$$

$$E_e = E_Z + T$$

$$E_f = \frac{1}{2}[E_D + E_Z - T] + \frac{1}{2}[(\Delta E_{ZD} - T)^2 + 8t^2]^{1/2}$$

where $\Delta E_{ZD} = E_Z - E_D$, E_g is the energy of the ground state, E_e is the energy of the singly excited state, and E_f is the energy of the doubly excited state. The eigen functions are

$$|\Psi_g\rangle = C_D{}^{1/2}|\Phi_D\rangle + \left(\frac{1 - C_D}{2}\right)^{1/2} \sum_{j=1}^{2} |\Phi_{Zj}\rangle$$

$$|\Psi_e\rangle = -2^{-1/2}(|\Phi_{Z1}\rangle - |\Phi_{Z2}\rangle)$$

$$|\Psi_f\rangle = (1 - C_D)^{1/2}|\Phi_D\rangle - \left(\frac{C_D}{2}\right)^{1/2} \sum_{j=1}^{2} |\Phi_{Zj}\rangle$$

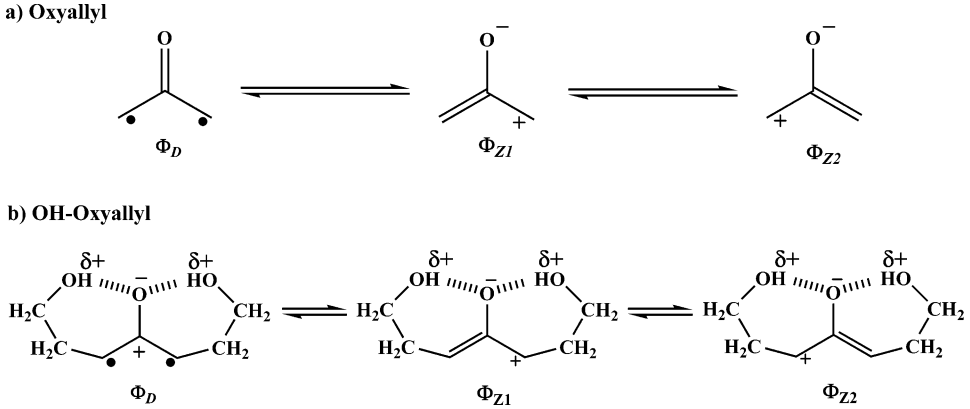

Figure 7. Resonance in the diradical and two zwitterionic forms states of oxyallyl and OH-oxyallyl substructures. Please note that in the OH-oxyallyl case, the zwitterionic character is retained in Φ_D.

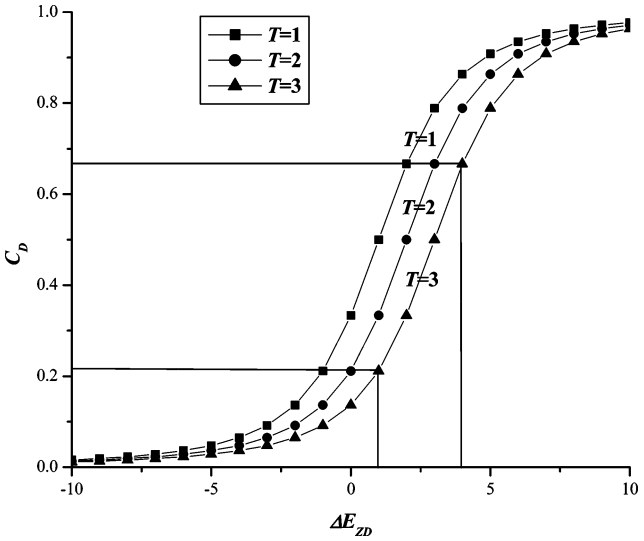

Figure 8. Variation of ΔE_{ZD} with diradical character (C_D) at different coupling constants between the two zwitterionic forms (T) at constant $t = 1.0$.

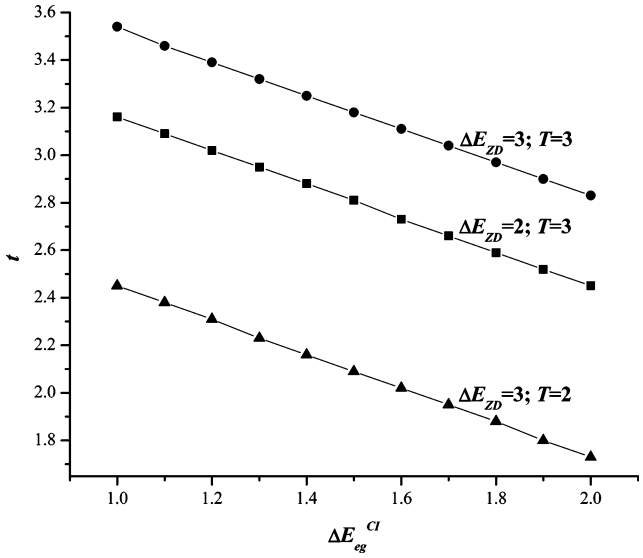

Figure 9. Variation of ΔE_{eg}^{CI} with coupling between diradical and zwitterionic forms (t) at constant coupling between the two zwitterionic forms (T) and constant ΔE_{ZD}.

The coefficient of the diradical form Φ_D can be considered as the diradical contribution. Hence the diradical character of the ground state can be represented as in terms of ΔE_{ZD}, T and t as

$$C_D = \frac{1}{2} + \frac{(\Delta E_{ZD} - T)}{2\sqrt{(\Delta E_{ZD} - T)^2 + 8t^2}} \tag{7}$$

The range of the ground state diradical character is from 0 to 1.0. The variation of the diradical character with the ΔE_{ZD} is shown in Figure 8. We show this variation for three values of T, namely $T = 1-3$ (at fixed $t = 1.0$). At large diradical character the ΔE_{ZD} is positive, indicating that the E_D is more stabilized than E_Z. On the other hand, for very small diradical character (below 0.2), the E_Z is more stabilized. Though the variation is also shown for the case when ΔE_{ZD} is negative, here due to large and intermediate diradical character, the ΔE_{ZD} will always be regarded as positive. As the T value decreases, one observes that the diradical character increases. This implies that as the interaction integral between the zwitterionic forms decreases, the diradical character increases. On the other hand, the diradical character can also increase at constant T with an increase of ΔE_{ZD}. Or, in other words, the larger diradical character case has a larger ΔE_{ZD} for the same coupling T, or smaller T at constant ΔE_{ZD}, at the same t.

Transition Energy and Transition Dipole Moments. We derive the transition energy of the lowest singlet state and the transition dipole, which is seen to be

$$\Delta E_{eg}^{CI} = E_e - E_g = \frac{\Delta E_{ZD} + 3T + [(\Delta E_{ZD} - T)^2 + 8t^2]^{1/2}}{2} \tag{8}$$

$$\mu_{g,e} = \langle \Psi_g | \hat{\mu} | \Psi_e \rangle \equiv \left(\frac{C_D}{2}\right)^{1/2} (\mu_{DZ2} - \mu_{DZ1}) + \frac{(1 - C_D)^{1/2}}{2} (\mu_{Z1Z2} - \mu_{Z2Z1} + \mu_{Z2} - \mu_{Z1}) \tag{9}$$

Using eq 8 we calculate the CI energy at fixed ΔE_{ZD} and T. This is shown graphically in Figure 9. We notice that if ΔE_{ZD} is constant and T reduces (larger diradical character), then the coupling, t, between the zwitterionic form and diradical form even with a small value shows an absorption in the red. On the other hand, for a fixed T and reduction of ΔE_{ZD}, again a small coupling t and the ΔE^{CI} can be in the red region. To put it in other words, even with a small increase in ΔE_{ZD} and a small decrease in T (which occurs with geometry perturbation), if coupling t is quite large, we could expect a red shift. In our case in the OH-oxyallyl diradical, the diradical and zwitterionic

structures share the zwitterionic characteristics; hence a large coupling, *t*, can be expected. Thus even for a smaller diradical character one can see the absorption in the NIR region.

For the transition dipole moment, eq 9 is slightly complicated. But if one neglects the cross terms (small values), then it can be seen that an increase in the diradical character decreases the transition dipole moments. As the OH-oxyallyl has a smaller diradical character, we can infer that the transition dipole moment will be larger. In other words, the small ΔE^{CI} and reasonably large μ leads to large γ. Thus we note here that the three-state model is sufficient to explain our observations.

Conclusions

OH-oxyallyl based systems have a larger C−O bond length and due to the H-bonding, a zwitterionic character is retained in the diradical VB form. This is absent in the case of oxyallyl substructure. Though both substructures have diradical character, in the case of the OH-oxyallyl system the singlet is the ground state due to the lower diradical character. Increasing the diradical nature in both cases by increasing the $C_3-C_2-C_{3'}$ bond angle reveals a red shift in absorption. But in the case of OH-oxyallyl even with small diradical character the absorption in the red is achieved. For the oxyallyl, the absorption in the red is seen with a large diradical character, but this could cause instability to the system. From the VB-3 state model, we infer that due to larger coupling between the diradical VB form and zwitterionic VB form, the OH-oxyallyl has not only an absorption in the red even with small diradical character but also a large transition dipole moment. Overall, this leads to large γ values with a negative sign. Because the BM4i4i dye is also a derivative of the OH-oxyallyl substructure, a similar absorption in the red and large γ value is obtained. This can be used as a design principle in oxyallyl systems in which diradical VB form can be forced to have large zwitterionic character for larger coupling between the two states leading to intense absorption and subsequently large NLO activity.

Acknowledgment. We are very much thankful to The Director, IICT, and to The Head, Inorganic Chemistry Division, IICT, for their constant support in this work. We also thank DST, New Delhi for the funding. K.Y. thanks CSIR for the fellowship. IICT Communication number: 070115.

Supporting Information Available: Tables of geometrical parameters, frequencies, and hyperpolarizabilities. This material is available free of charge via the Internet at http://pubs.acs.org.

References and Notes

(1) Fabian, J. *Chem. Rev.* **1992**, *92*, 1197−1228.

(2) Fabian, J.; Zahradnik, R. *Angew. Chem. Int. Ed.* **1989**, *28*, 677−694.

(3) Law, K. Y. *Chem. Rev.* **1993**, *93*, 449.

(4) (a) *IR absorbing Dyes*; Matsuoka, M., Ed.; Plenum Press: New York, 1990. (b) *Near-Infrared Dyes for High Technology Applications*; NATO ASI Series 3; Daehne, S., Resch-Genger, U., Wolfbeis, O. S., Eds.; Kluwer Academic: Dordrecht, The Netherlands, 1998; Vol. 52, ISBN 0.7923-5101-0.

(5) Tian, M.; Tatsuura, S.; Furuki, M.; Sato, Y.; Iwasa, I.; Pu, L. S. *J. Am. Chem. Soc.* **2003**, *125*, 348−349.

(6) Tatsuura, S.; Tian, M.; Furuki, M.; Sato, Y.; Iwasa, I.; Mitsu, H. *Appl. Phys. Lett.* **2004**, *84*, 1450−1452.

(7) Tatsuura, S.; Mastubara, T.; Tian, M.; Mitsu, H.; Iwasa, I.; Sato, Y.; Furuki, M. *Appl. Phys. Lett.* **2004**, *85* (4), 540−542.

(8) Langhals, H. *Angew. Chem. Int. Ed.* **2003**, *42*, 4286−4288.

(9) könig, W. *J. Prakt. Chem.* **1925**, *112*, 1−36.

(10) Ismailsky, W. Dissertation, Universität Dresden, 1913.

(11) Dilthey, W.; Wizinger, R. *J. Prakt. Chem.* **1928**, *118*, 321−348.

(12) Wizinger, R. *Chimia* **1961**, *15*, 89−105.

(13) Griffiths, J. *Colour and Constitution of Organic Molecules*; Academic Press: London, 1976; ISBN 0-12-303550-3, LCCC 76-016971.

(14) Dähne, S.; Kulpe, S. *Structural Principles of Unsaturated Organic Compounds*; Akademic Verlag: Berlin, 1977 (Abh. Akad. Wiss. DDR No. 8).

(15) Dewar, M. J. S.; Dougherty, R. C. *The PMO Theory of Organic Chemistry*, 1st ed.; Plenum: New York, 1975; pp 410−418, ISBN 0-306-20010-4.

(16) (a) Prabhakar, Ch.; Krishna Chaitanya, G.; Sitha, S.; Bhanuprakash, K.; Jayathritha Rao, V. *J. Phys. Chem. A* **2005**, *109*, 2614. (b) Prabhakar, Ch.; Yesudas, K.; Krishna Chaitanya, G.; Sitha, S.; Bhanuprakash, K.; Jayathritha Rao, V. *J. Phys. Chem. A* **2005**, *109*, 8604. (c) Yesudas, K.; Krishna, C. G.; Prabhakar, Ch.; Bhanuprakash, K.; Jayathritha Rao, V. *J. Phys. Chem. A* **2006**, *110*, 11717.

(17) Fann, W. S.; Benson, S.; Madey, J. M. J.; Etemad, S.; Baker, G. L.; Kajzar, F. *Phys. Rev. Lett.* **1989**, *62*, 1492.

(18) (a) LI, Z.; Jin, Z. H.; Kasatani, K.; Okamoto, H.; Takenaka, S. *Jpn. J. Appl. Phys.* **2005**, *44*, 4956. (b) LI, Z.; Jin, Z. H.; Kasatani, K.; Okamoto, H. *Physica B* **2006**, *382*, 229.

(19) Bredas, J. L.; Adant, C.; Tackx, P.; Persoons, A.; Pierce, B. M. *Chem. Rev.* **1994**, *94*, 243 and references cited therein.

(20) Nakano, M.; Kishi, R.; Ohta, S.; Takebe, A.; Takahashi, H.; Furukawa, S.; Takashi, K.; Morita, Y.; Nakasuji, K.; Yamaguchi, K.; Kamada, K.; Ohta, K.; Champagne, B.; Botek, B. *J. Chem. Phys.* **2006**, *125*, 74113.

(21) (a) Nakano, M.; Takashi, K.; Kamada, K.; Ohta, K.; Kishi, R.; Ohta, S.; Nakagawa, N.; Takahashi, H.; Furukawa, S.; Morita, Y.; Nakasuji, K.; Yamaguchi, K. *Chem. Phys. Lett.* **2006**, *418*, 142. (b) Ohta, S.; Nakano, M.; Takashi, K.; Kamada, K.; Ohta, K.; Kishi, R.; Nakagawa, N.; Champagne, B.; Botek, E.; Umezaki, S.; Takebe, A.; Takahashi, H.; Furukawa, S.; Morita, Y.; Nakasuji, K.; Yamaguchi, K. *Chem. Phys. Lett.* **2006**, *420*, 432. (c) Nakano, M.; Nakagawa, N.; Ohta, S.; Kishi, K.; Takashi, K.; Kamada, K.; Ohta, K.; Champagne, B.; Botek, E.; Takahashi, H.; Furukawa, S.; Morita, Y.; Nakasuji, K.; Yamaguchi, K. *Chem. Phys. Lett.* **2006**, *429*, 174.

(22) Frisch, M. J.; Trucks, G. W.; Schlegel, H. B.; Scuseria, G. E.; Robb, M. A.; Cheeseman, J. R.; Montgomery, J. A., Jr.; Vreven, T.; Kudin, K. N.; Burant, J. C.; Millam, J. M.; Iyengar, S. S.; Tomasi, J.; Barone, V.; Mennucci, B.; Cossi, M.; Scalmani, G.; Rega, N.; Petersson, G. A.; Nakatsuji, H.; Hada, M.; Ehara, M.; Toyota, K.; Fukuda, R.; Hasegawa, J.; Ishida, M.; Nakajima, T.; Honda, Y.; Kitao, O.; Nakai, H.; Klene, M.; Li, X.; Knox, J. E.; Hratchian, H. P.; Cross, J. B.; Adamo, C.; Jaramillo, J.; Gomperts, R.; Stratmann, R. E.; Yazyev, O.; Austin, A. J.; Cammi, R.; Pomelli, C.; Ochterski, J. W.; Ayala, P. Y.; Morokuma, K.; Voth, G. A.; Salvador, P.; Dannenberg, J. J.; Zakrzewski, V. G.; Dapprich, S.; Daniels, A. D.; Strain, M. C.; Farkas, O.; Malick, D. K.; Rabuck, A. D.; Raghavachari, K.; Foresman, J. B.; Ortiz, J. V.; Cui, Q.; Baboul, A. G.; Clifford, S.; Cioslowski, J.; Stefanov, B. B.; Liu, G.; Liashenko, A.; Piskorz, P.; Komaromi, I.; Martin, R. L.; Fox, D. J.; Keith, T.; Al-Laham, M. A.; Peng, C. Y.; Nanayakkara, A.; Challacombe, M.; Gill, P. M. W.; Johnson, B.; Chen, W.; Wong, M. W.; Gonzalez, C.; Pople, J. A. *Gaussian 03*, revision 01; Gaussian, Inc.: Wallingford, CT, 2004.

(23) (a) Nakajima, T.; Nakatsuji, H. *Chem. Phys. Lett.* **1997**, *280*, 79. (b) Ishida, M.; Toyota, K.; Ehara, M.; Nakatsuji, H. *Chem. Phys. Lett.* **2001**, *347*, 493. (c) Nakajima, T.; Nakatsuji, H. *Chem. Phys. Lett.* **1999**, *242*, 177. (d) Nakajima, T.; Nakatsuji, H. *Chem. Phys. Lett.* **1999**, *300*, 1. (e) Wan, Jian.; Ehara, M.; Hada, M.; Nakatsuji, H. *J. Chem. Phys.* **2000**, *113*, 5245. (f) Wan, J.; Hada, M.; Ehara, M.; Nakatsuji. M. *J. Chem. Phys*. **2001**, *114* (*2*), 842. (g) Nakatsuji, H. Models in Chemistry. *Acta Chim. Hung.* **1992**, *129*, 719. (h) Nakatsuji, H. In *Computational Chemistry- Reviews of Current Trends*; Leszczynski, J., Ed.; World Scientific: Singapore, 1997; Vol. 2.

(24) Hrovat, D. A.; Murcko, M. A.; Lahit, P. M.; Borden, W. T. *J. Chem. Soc., Perkin Trans.* **1998**, *2*, 1037.

(25) Schalleya, C. H.; Stephen, B.; Jeremy, N. H.; Detlef, S.; Waltraud, Z.; John, H. B.; Schwarz, H. *Eur. J. Org. Chem.* **1998**, 987.

(26) Hess, B. A., Jr.; Smentek, L. *Eur. J. Org. Chem.* **1999**, 3363.

(27) (a) Wirz, J. *Pure Appl. Chem.* **1984**, *56*, 1289. (b) Dohnert, D.; Koutecky, J. *J. Am. Chem. Soc.* **1980**, *102*, 1790.

(28) Nakano, M.; Nitta, T.; Yamaguchi, K.; Champagne, B.; Botek, E. *J. Phys. Chem. A* **2004**, *108*, 4105.

(29) Yamaguchi, K. In *Self-Consistent Field Theory and Applications*; Carbo, R., Klobukowski, M., Eds.; Elsevier: Amsterdam, 1990; p 727.

(30) Yamanaka, S.; Okumura, M.; Nakano, M.; Yamaguchi, K. *J. Mol. Struct. (THEOCHEM)* **1994**, *310*, 205.

(31) (a) Bachler, V.; Olbrich, G.; Neese, F.; Wieghardt, K. *Inorg. Chem.* **2002**, *41*, 4179. (b) Adamo, C.; Barone, V.; Bencini, A.; Totti, F.; Ciofini, I. *Inorg. Chem.* **1999**, *38*, 1996.

(32) Salem, L.; Rowland, C. *Angew. Chem. Int. Ed.* **1972**, *11*, 92.

(33) Michl, J.; Bonacic-Koutecky, V. *Tetrahedron* **1988**, *44*, 7559.

(34) Koutecky, V. B.; Koutecky, J.; Michl, J. *Angew. Chem. Int. Ed.* **1987**, *26*, 170.

(35) (a)Kamada, K.; Ueda, M.; Nagao, H.; Tawa, K.; Takushi, S.; Shmizu, Y.; Ohta, K. *J. Phys. Chem. A* **2000**, *104*, 4723 and references cited therein. (b) Kurtz, H. A.; James Stewart, J. P.; Dieter, K. M. *J. Comput. Chem.* **1990**, *11*, 82.

(36) Cho, M.; An, S. Y.; Lee, H.; Ledoux, I.; Zyss, J. *J. Chem. Phys.* **2002**, *116*, 9165.

(37) Cho, M.; Kim, H. S.; Jeon, S. J. *J. Chem. Phys.* **1998**, *108*, 7114.

(38) Barzoukas, M.; Blanchard-Desce, M. *J. Chem. Phys.* **2000**, *113*, 3951.

(39) Lee, Y. K.; Jeon, S. J.; Cho, M. *J. Am. Chem. Soc.* **1998**, *120*, 10921.

(40) Lee, H.; An, S. Y.; Cho, M. *J. Phys. Chem. B* **1999**, *103*, 4992.

(41) Cho, M. *J. Phys. Chem. A* **1999**, *103*, 4712.

(42) Lu, D.; Chen, G.; Perry, J. W.; Goddard, W. A., III. *J. Am. Chem. Soc.* **1994**, *116*, 10679.